
Adaptation of retinal processing to image contrast and spatial scale

**Stelios M. Smirnakis^{*†}, Michael J. Berry[‡],
David K. Warland[‡], William Bleak[§] & Markus Meister[‡]**

Departments of Physics, and ‡ Molecular and Cellular Biology,
Harvard University, 16 Divinity Avenue, Cambridge, Massachusetts 02138, USA
† Division of Health Sciences and Technology, Harvard Medical School,
260 Longwood Avenue, Boston, Massachusetts 02115, USA
§ NEC Research Institute, Princeton, New Jersey 08540, USA*

Owing to the limited dynamic range of a neuron's output, neural circuits are faced with a trade-off between encoding the full range of their inputs and resolving gradations among those inputs. For example, the ambient light level varies daily over more than nine orders of magnitude¹, whereas the firing rate of optic nerve fibres spans less than two². This discrepancy is alleviated by light adaptation³: as the mean intensity increases, the retina becomes proportionately less sensitive. However, image statistics other than the mean intensity also vary drastically during routine visual processing. Theory predicts that an efficient visual encoder should adapt its strategy not only to the mean, but to the full shape of the intensity distribution⁴⁻⁶. Here we report that retinal ganglion cells, the output neurons of the retina, adapt to both image contrast—the range of light intensities—and to spatial correlations within the scene, even at constant mean intensity. The adaptation occurs on a scale of seconds, one hundred times

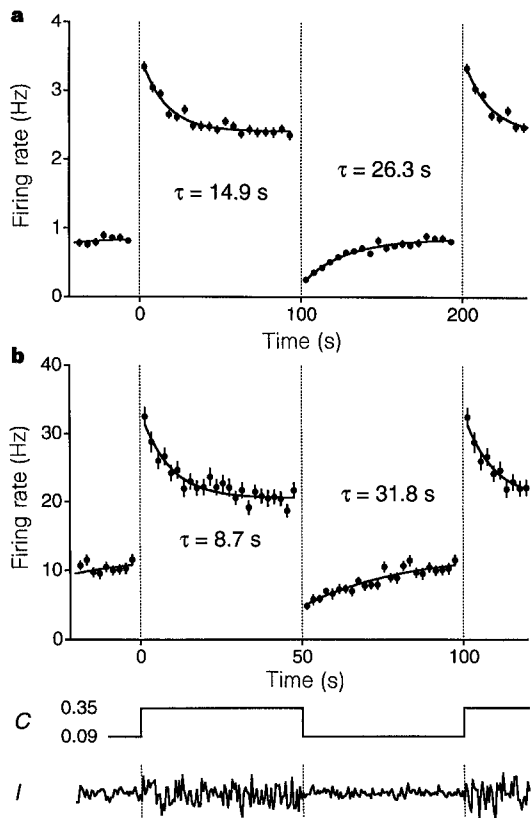


Figure 1 Firing rate of a salamander (a) and a rabbit (b) ganglion cell under spatially uniform flicker stimulation, alternating every 100 (a) or 50 (b) seconds between contrast values of 0.09 and 0.35. Average firing rate values were computed in 5-s (a) or 2-s (b) time bins over 100 (a) or 25 trials (b). Continuous lines are exponential fits with decay time τ . The first and last segments are periodic repeats of the data. Trace below (b) shows the time course of the contrast, C. Bottom trace illustrates the time course of the flickering intensity, I; note that the random flicker sequence was different in each stimulus trial. Similar gradual changes in the firing rate were unambiguous in 75% of salamander and 51% of rabbit cells. Another 18% in salamander and 31% in rabbit showed the gradual firing rate decline after a contrast increase but no detectable recovery following a contrast decrease.

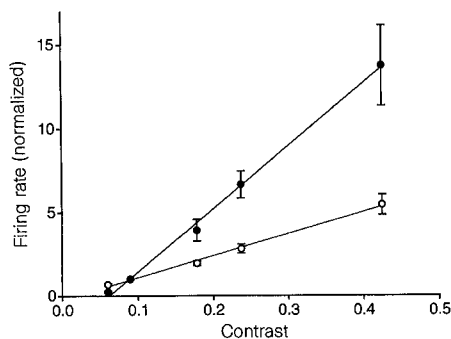


Figure 2 Initial firing rate (R_i , closed symbols) and final firing rate (R_f , open symbols) following a contrast step from $C = 0.09$ to values ranging between 0.06 and 0.43. For each cell, R_i and R_f were calculated as in Table 1 and normalized to yield $R_i = 1$ at $C = 0.09$, then averaged over 53 salamander ganglion cells from 2 retinæ. Lines are linear fits.

more slowly than the immediate light response, and involves 2–5-fold changes in the firing rate. It is mediated within the retinal network: two independent sites of modulation after the photoreceptor cells appear to be involved. Our results demonstrate a remarkable plasticity in retinal processing that may contribute to the contrast adaptation of human vision⁷.

We recorded the spike trains of ganglion cells in the isolated retina of a tiger salamander or rabbit. The photoreceptor layer was presented with random flicker stimuli whose mean intensity remained constant throughout, but whose second-order statistics changed abruptly at long intervals (see Methods). The goal was to monitor changes in retinal processing that are brought about by such a switch in the properties of the artificial visual environment. The first set of experiments employed a spatially uniform flickering field; its mean intensity was kept constant, but the width of the intensity distribution increased or decreased abruptly. Following such a step increase in contrast, the firing rate of most retinal ganglion cells increased abruptly, then decayed exponentially to a much lower value (Fig. 1 and Table 1). Following the opposite contrast step, the firing rate dropped abruptly and then recovered exponentially. These gradual changes in the firing rate suggest an adaptive modification of ganglion cell response properties following a step in contrast. For most salamander cells, the decay of the firing rate after a contrast increase was 2 to 3 times faster than its recovery following a contrast decrease (Table 1). Rabbit ganglion cells adapted very similarly (Fig. 1b and Table 1), even though their absolute firing rates were an order of magnitude higher than those of salamander ganglion cells. ‘On’ and ‘off’ cells showed no qualitative differences in their adaptation behaviour to this stimulus.

The initial firing rate immediately following a contrast jump

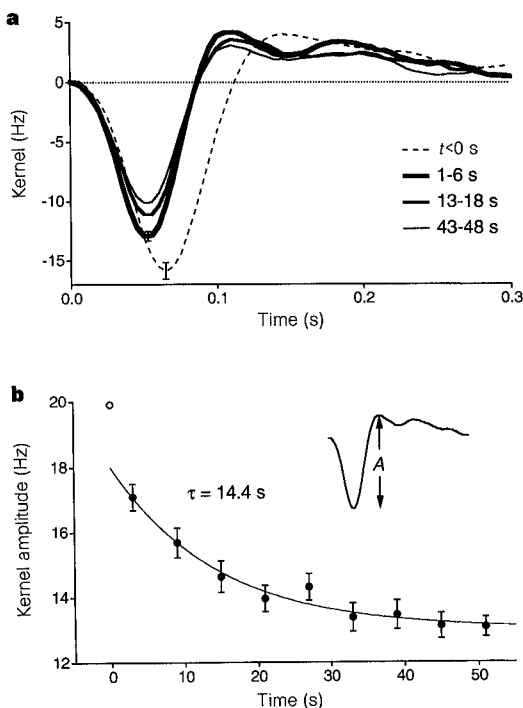


Figure 3 a, The effect of a contrast step from $C = 0.09$ to 0.35 on the linear kernel of a salamander ganglion cell (from Fig. 1a): just before the step (broken line), after the step at 1–6 s (thick line), 13–18 s (medium line), and 43–48 s (thin line). The kernel $k(t)$ was computed with 5-ms bins over the respective time interval and averaged over 50 stimulus trials (see Methods). **b**, Peak-to-peak amplitude (inset) of the kernel from the cell in (a), as a function of time relative to the contrast transition. Open symbol represents value at $t < 0$. Continuous line is an exponential fit to data after the step, with decay time τ . A similar decrease of the kernel amplitude was observed in 93% of salamander and 85% of rabbit cells.

increased linearly with the final contrast (Fig. 2). The steady-state firing rate, after the exponential transient, also varied linearly with the contrast. However, the latter curve was less than half as steep as the former, a clear sign of contrast adaptation. Using the same criterion, but different stimuli, a small but significant contrast adaptation effect has been demonstrated in the cat's lateral geniculate nucleus⁸.

To determine how each ganglion cell responded to the flickering light, we computed the linear kernel of its firing rate with respect to the stimulus intensity^{9,10}; this can also be viewed as the linear response to a brief flash of light (see Methods). A step increase in contrast triggered a rapid change in the shape of this kernel towards a faster waveform (Fig. 3a, broken and thick lines). This was followed by a gradual decrease of the kernel amplitude (Fig. 3 and Table 1). Following the opposite contrast step, the kernel shape reverted and its amplitude gradually increased. The fact that the slow changes in kernel amplitude and firing rate occur with a very similar time course (Figs 1a and 3b) suggests that the rate modulations truly reflect a change in the sensitivity of the light response. At low contrast, a high sensitivity serves to represent effectively the narrow range of intensities. Following a sudden transition to high contrast, the sensitivity gradually decreases to encode the broader intensity range.

Previous studies of retinal signalling in cat¹¹ and catfish⁹ indicated that ganglion cell response properties change as a function of ambient contrast. This 'contrast gain control' occurred within tens of milliseconds¹² of a contrast step, which is less than the photoreceptor integration time. Figure 3a also shows a shift of ganglion cell sensitivity towards higher temporal frequencies that occurs immediately after the contrast step, as seen in cat¹¹. These fast changes can be viewed as a nonlinear feature of the instantaneous

light response¹³, rather than as gradual adaptation to scene statistics. By comparison, the subsequent adaptation phase documented here requires seconds to tens of seconds. This is similar to the time in which an animal might move into an environment of substantially different texture, or in which the scene illumination might change from direct to diffuse light, producing a change in contrast.

Some neural element within the retina must sense the contrast and control the change in sensitivity. To estimate the size of this neuron's receptive field, we stimulated the salamander retina alternately with a flickering checkerboard of varying square size, D , and spatially uniform flicker of the same mean and contrast (see Methods). Under these conditions, only neurons whose receptive field extended over more than one square of the checkerboard experienced a change in the statistics of their synaptic input as a result of the transition to uniform flicker.

Figure 4a illustrates the firing rate of a salamander ganglion cell in such an experiment. Following a transition from uniform to checkerboard stimulation, the firing rate suddenly increased, then gradually declined over several seconds to a steady state. Following the reverse transition, the firing rate suddenly decreased, then gradually recovered. Judging from the final steady-state firing rate, the neuron was driven more strongly by checkerboards than by uniform fields, consistent with the centre-surround antagonism in its receptive field. During the adaptation phase, the neuron's sensitivity always declined when exposed to a stronger stimulus, and recovered under a weaker stimulus, analogous to the observations with uniform stimulation at varying contrast (Fig. 1). Thus, the same mechanism may account for both observations (Fig. 5). Such behaviour was seen in all 'on' cells.

However, the great majority of 'off' ganglion cells behaved like the neuron shown in Fig. 4b. During the adaptation phase the neuron's

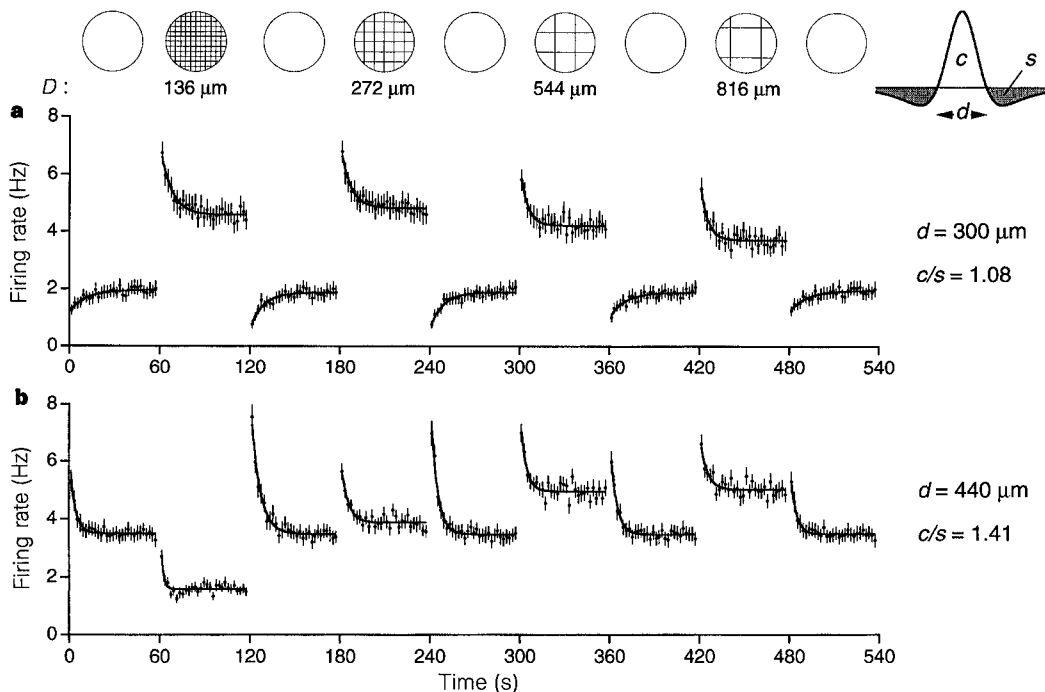


Figure 4 Adaptation to a change in spatial scale for two salamander ganglion cells, 'on' type (a) and 'off' type (b). Top row illustrates time course of the stimulus during a trial, alternating between uniform and checkerboard stimulation at varying square size, D . The checkerboard was also shifted every 30 ms by a spatial offset chosen at random on a 136- μm grid; this ensured that checkerboard boundaries would not consistently fall on the same neural receptive fields. Contrast remained at $C = 0.24$ throughout. Average firing rates were computed in 2-s intervals over 50 trials. Lines are exponential fits. The last data segment (480–540 s) is identical to the first (0–60 s). The receptive field profiles (see Methods) of

both cells are summarized (right) by the diameter of the centre region, d , and the ratio of integrated sensitivity in the positive centre to that in the negative surround, c/s . Note that the steady-state firing rates are maximal when $D \approx d$, and are suppressed more under uniform illumination when the surround is stronger, as in a. 12% of recorded neurons showed adaptation as in a, 82% as in b; for 6% the firing rate adapted downwards only following the transition from uniform to checkerboard stimulation. In the rabbit retina these stimuli produced qualitatively similar adaptation of the ganglion cell firing rate, but there was no sharp distinction between 'on' and 'off' cells.

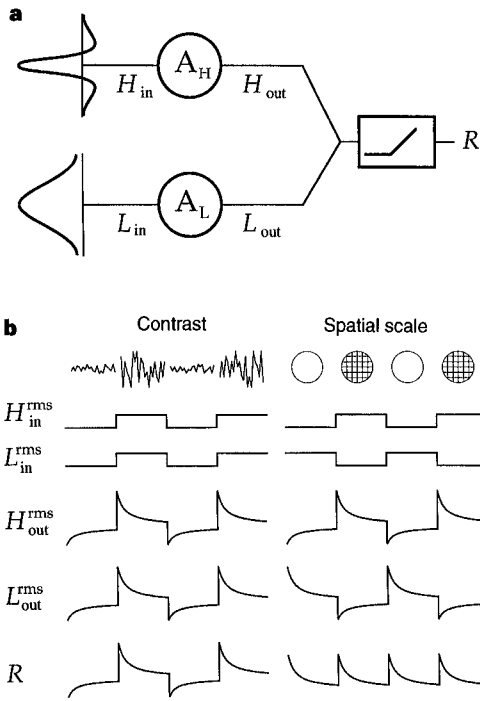


Figure 5 a, Model of contrast adaptation. Two pathways lead from the stimulus to the ganglion cell: one (H, 'high pass') integrates the stimulus with a spatially antagonistic receptive field; the other (L, 'low pass') has a broad receptive field. Each pathway contains an adaptive neuron (A_H , A_L) which gradually increases its sensitivity when its input signal (H_{in} , L_{in}) varies over a small range, and gradually decreases its sensitivity when its input range is large. The output signals of the two pathways (H_{out} , L_{out}) are pooled and rectified to produce a positive ganglion cell firing rate (R). **b**, Predictions for the firing rate under variations in contrast (left) or checkerboard-square size (right). The range of signals in the H and the L pathways are indicated by their root-mean-square variations, H^{rms} and L^{rms} . When the flicker contrast is stepped up (left), both pathways are driven more strongly and thus adapt by decreasing their sensitivity, resulting in a gradual decline in the firing rate. The opposite is predicted when the contrast steps down. When switching from uniform to checkerboard stimulation (right), the H pathway is driven more strongly and the L pathway more weakly. Thus their sensitivities adapt in the opposite direction. As the downward adaptation transients are larger than the upward transients (Fig. 1), the net effect is a gradual decline of the firing rate. When switching back to uniform stimulation, the roles of H and L pathways are switched, but their pooled activity again results in a gradual decline of the firing rate. This can explain the behaviour of salamander 'off' cells in Fig. 1a (left) and Fig. 4b (right). 'On' cells behave as though they lack the L pathway, or at least its adaptive control, because their firing rate under both conditions (Figs 1a and 4a) varies as the output signal in the H pathway.

Table 1 Characteristics of adaptation transients induced by changes in contrast

	Contrast		τ (s)		R_i/R_f		A_i/A_f	
	C_{low}	C_{high}	↑	↓	↑	↓	↑	↓
Salamander	0.06	0.18	9.1 ± 0.9 (44)	17.8 ± 1.7 (24)	2.48 ± 0.31 (44)	0.18 ± 0.04 (24)	1.48 ± 0.07 (42)	0.56 ± 0.06 (17)
	0.09	0.35	8.8 ± 1.1 (20)	28.5 ± 2.7 (17)	1.69 ± 0.14 (20)	0.37 ± 0.06 (17)	1.26 ± 0.05 (20)	0.60 ± 0.07 (16)
Rabbit	0.09	0.35	12.6 ± 1.28 (36)	27.3 ± 2.7 (16)	2.26 ± 0.27 (36)	0.27 ± 0.06 (16)	1.45 ± 0.13 (29)	0.68 ± 0.07 (16)

Changes in contrast from C_{low} to C_{high} are indicated by an upward arrow, and from C_{high} to C_{low} by a downward arrow. For each cell, the time course of the firing rate was fitted with an exponential of time constant τ (Fig. 1) and extrapolated to yield the initial and final firing rate, R_i and R_f . The kernel amplitude, A , was taken as the peak-to-peak amplitude of the waveform (Fig. 3b), and its initial and final values, A_i and A_f , were measured over the first and the last 5-s interval of the contrast segment respectively. The parameters τ , R_i/R_f , and A_i/A_f were averaged over all cells that showed adaptation (Figs 1 and 3), except when τ or A could not be determined accurately. The number of cells for each estimate is given in parentheses. Uncertainties denote standard error.

sensitivity was initially high and gradually declined following every stimulus transition, irrespective of whether the final rate increased or decreased. In fact, the final rate under 272- μ m squares was almost identical to that under uniform stimulation, yet the transition produced a large transient during which the rate changed by more than a factor of two. This behaviour cannot be explained by a single mechanism of local contrast adaptation, but could result from independent adaptation in two pathways, one of which responds best at high spatial frequencies, the other at low frequencies (Fig. 5).

In these experiments, both the mean and the local contrast were held constant, and the adaptation process was triggered purely by a change in the spatial scale of the scene. These results place strong constraints on the site of adaptation. In particular, it does not occur in photoreceptors: The receptive field of cones—including their electrical coupling which extends over $\sim 25 \mu$ m in turtle¹⁴—is too small to detect the difference between checkerboard and uniform stimulation. In the scheme proposed in Fig. 5, the H pathway must have a narrow centre, with a large surround extending over more than 800 μ m (the largest square size tested). Bipolar cells—with their broad antagonistic surrounds from the horizontal cell syncytium^{15,16}—could serve this role, as could the ganglion cell itself. The L pathway could be implemented by wide-field amacrine cells in the inner retina^{17,18}. These assignments and the scheme in Fig. 5 are tentative, but they provide one framework for explaining the contrast adaptation behaviour of ganglion cells.

The effects reported here share several characteristics with contrast adaptation observed in human subjects and in the responses of cortical neurons. After adapting to a drifting grating, the threshold

for detecting a similar test grating is raised about 5-fold⁷, comparable in magnitude to the observed changes in the firing rate of retinal ganglion cells (Table 1, and see ref. 19). The time constants of psychophysical contrast adaptation also range from second to tens of seconds^{7,20}. The loss of sensitivity after a contrast increase and the recovery after a contrast decrease often follow a different time course^{21–23}, a consistent feature in our recordings (Fig. 1 and Table 1; $P < 0.001$). Although this suggests that retinal processing is important in psychophysical contrast adaptation, cortical mechanisms certainly contribute as well, because there is partial interocular transfer of adaptation^{7,20,24} and neurons in the cat visual cortex adapt more strongly to grating stimuli than neurons in the lateral geniculate nucleus⁸.

In summary, it appears that visual processing in the retina is considerably more adaptive than previously acknowledged and adjusts not only to the mean illumination but also to both the range of intensity fluctuations and their spatial scale. Essentially identical behaviour was observed in a mammalian and an amphibian species, and related effects are seen in an insect visual system⁵, suggesting that this strategy is a general principle of retinal processing. More broadly, it might be expected that any neural circuit would benefit from an adaptive control that responds to changes in the statistics of its inputs. The retina, with its accessible and well studied circuitry, is ideal for studying the underlying mechanisms. □

Methods

Recording. Retinae of larval tiger salamanders and Dutch belted rabbits were isolated in darkness into oxygenated Ringer's medium¹⁰ (salamander) or Ames'

solution (rabbit; Sigma A-1420 supplemented with 22.6 mM Na_2HCO_3 , 4.4 mM D-glucose, pH 7.4; maintained at 37 °C during recording). A piece of retina 2–4 mm on a side was placed onto a flat multi-electrode array for extracellular recording from the ganglion cell layer^{10,25}. Results are reported from 71 cells in 4 salamander retinas, 55 cells in 2 rabbit retinas (Figs 1, 2, 3; Table 1), and 33 cells in 2 salamander retinas (Fig. 4). In the salamander, 14% of recorded ganglion cells were 'on' and 86% 'off'. In the rabbit, 33% were 'on', 51% 'off', and 16% had mixed response properties.

Stimulation. Stimuli were projected from a computer monitor onto a 3.25-mm-diameter aperture on the retina. Patterns consisted of a single uniform field of flickering light (Figs 1–3) or a flickering checkerboard with independently modulated square fields (Fig. 4), ranging in size, D , from 0.068 to 0.816 mm. The light intensity of each field was chosen every $\Delta t = 30$ ms at random from a gaussian probability distribution with mean M and standard deviation W . Contrast, C , was defined as W/M . The field size D sets the spatial scale of the stimulus. All experiments used white light²⁶ with a mean intensity of $M = 4.2 \text{ mW m}^{-2}$ at the retina. The equivalent photon flux at the peak absorption wavelength (λ_{max}) was $5,680 \text{ photons } \mu\text{m}^{-2} \text{ s}^{-1}$ for the salamander's red cone photoreceptor ($\lambda_{\text{max}} = 630 \text{ nm}$), and $5,150 \text{ photons } \mu\text{m}^{-2} \text{ s}^{-1}$ for the rabbit's green cone ($\lambda_{\text{max}} = 523 \text{ nm}$)^{27,28}.

Analysis. In a typical experiment, we interleaved segments of two stimulus types in the order $A_1B_1A_2B_2A_3B_3\dots$, where the A_i represents segments with the same contrast and spatial scale, but different random flicker sequences, and B_i represent segments with another contrast or spatial scale. Individual segments of A and B lasted either 50 s or 100 s, and recordings extended over 25 to 100 AB trials. The mean firing rate at a given time around the A-to-B transition (Figs 1, 2, 4) was computed by counting the spikes in the corresponding short time bin of all the AB trials, and dividing by the number of trials and the length of the time bin. The first-order Wiener kernel (Fig. 3) of the response was computed by correlating the stimulus intensity $I(t)$ and the firing rate $R(t)$: $k(t) = \frac{1}{WC} \frac{1}{T} \int_0^T (I(t') - M)R(t' + t)dt'$. This represents the linear effect on the firing rate from a flash of light with integrated intensity $M \cdot \Delta t$. The kernel at a given time around the transition was computed by performing the integral only over the corresponding time bins of all individual trials. The spatial receptive field (Fig. 4) was determined from steady-state responses to checkerboard stimulation with $136\text{-}\mu\text{m}$ squares: the kernel $k(t)$ was computed for each square, and its peak amplitude plotted as a function of position. All error bars in figures represent the standard error across trials.

Received 10 September 1996; accepted 9 January 1997.

1. Rushton, W. A. Visual Adaptation (The Ferrier Lecture, 1962). *Proc. R. Soc. Lond. B* **162**, 20–46 (1965).
2. Barlow, H. B. Critical limiting factors in the design of the eye and visual cortex (The Ferrier Lecture, 1980). *Proc. R. Soc. Lond. B* **212**, 1–34 (1981).
3. Shapley, R. & Enroth-Cugell, C. Visual Adaptation and Retinal Gain Controls. *Progr. Ret. Res.* **3**, 263–346 (1984).
4. Laughlin, S. A simple coding procedure enhances a neuron's information capacity. *Z. Naturforsch.* **36**, 910–912 (1981).
5. de Ruyter van Steveninck, R. R., Bialek, W., Potters, M. & Carlson, R. H. Statistical adaptation and optimal estimation in movement computation by the blowfly visual system. *Proc. IEEE Int. Conf. Systems, Man, and Cybernetics* 302–308 (1994).
6. DeWeese, M. & Bialek, W. Information flow in sensory neurons. *Il Nuovo Cimento* **17D**, 733–738 (1995).
7. Blakemore, C. & Campbell, F. W. On the existence of neurones in the human visual system selectively sensitive to the orientation and size of retinal images. *J. Physiol.* **203**, 237–260 (1969).
8. Ohzawa, I., Sclar, G. & Freeman, R. D. Contrast gain control in the cat's visual system. *J. Neurophysiol.* **54**, 651–667 (1985).
9. Sakai, H. M. & Naka, K. Signal transmission in the catfish retina. V. Sensitivity and circuit. *J. Neurophysiol.* **58**, 1329–1350 (1987).
10. Meister, M., Pine, J. & Baylor, D. A. Multi-neuronal signals from the retina: acquisition and analysis. *J. Neurosci. Meth.* **51**, 95–106 (1994).
11. Shapley, R. M. & Victor, J. D. The effect of contrast on the transfer properties of cat retinal ganglion cells. *J. Physiol.* **285**, 275–298 (1978).
12. Victor, J. D. The dynamics of the cat retinal X cell centre. *J. Physiol.* **386**, 219–246 (1987).
13. Wang, J.-L. & Naka, K.-I. Contrast gain control in the lower vertebrates retinas. *Soc. Neurosci. Abstr.* **21**, 1644 (1995).
14. Copenhagen, D. R. & Green, D. G. The absence of spread of adaptation between rod photoreceptors in turtle retina. *J. Physiol.* **369**, 161–181 (1985).
15. Dacheux, R. F. & Raviola, E. Horizontal cells in the retina of the rabbit. *J. Neurosci.* **2**, 1486–1493 (1982).
16. Hare, W. A. & Owen, W. G. Spatial organization of the bipolar cell's receptive field in the retina of the tiger salamander. *J. Physiol.* **421**, 223–245 (1990).
17. Werblin, F., Maguire, G., Lukasiewicz, P., Eliasof, S. & Wu, S. M. Neural interactions mediating the detection of motion in the retina of the tiger salamander. *Visual Neurosci.* **1**, 317–329 (1988).
18. Bloomfield, S. A. Relationship between receptive and dendritic field size of amacrine cells in the rabbit retina. *J. Neurophysiol.* **68**, 711–725 (1992).
19. Barlow, H. B. & Hill, R. M. Evidence for a physiological explanation of the waterfall phenomenon and figural after-effects. *Nature* **200**, 1345–1347 (1963).

20. Schieting, S. & Spillmann, L. Flicker adaptation in the peripheral retina. *Vision Res.* **27**, 277–284 (1987).
21. Albrecht, D. G., Farrar, S. B. & Hamilton, D. B. Spatial contrast adaptation characteristics of neurones recorded in the cat's visual cortex. *J. Physiol.* **347**, 713–739 (1984).
22. Ho, W. A. & Berkley, M. A. Evoked potential estimates of the time course of adaptation and recovery to counterphase gratings. *Vision Res.* **28**, 1287–1296 (1988).
23. Giaschi, D., Douglas, R., Marlin, S. & Cynader, M. The time course of direction-selective adaptation in simple and complex cells in cat striate cortex. *J. Neurophysiol.* **70**, 2024–2034 (1993).
24. Barlow, H. B. & Bridley, G. S. Inter-ocular transfer of movement aftereffects during pressure binding of the stimulated eye. *Nature* **200**, 1347 (1963).
25. Meister, M., Lagnado, L. & Baylor, D. A. Concerted signaling by retinal ganglion cells. *Science* **270**, 1207–1210 (1995).
26. Brainard, D. Calibration of a computer controlled color monitor. *Color Res. Appl.* **14**, 23–34 (1989).
27. Dawis, S. M. Polynomial expressions of pigment nomograms. *Vision Res.* **21**, 1427–1430 (1981).
28. Nuboer, J. F. W. & Moed, P. J. Increment-threshold spectral sensitivity in the rabbit. *J. Comp. Physiol.* **151**, 353–358 (1983).

Acknowledgements. We thank T. Jordan for help with rabbit experiments, the members of our group and B. Chang for discussion, and D. Baylor, J. Dowling, C. Reid, F. Rieke and J. Victor for comments on the manuscript. Supported by a grant from the Office of Naval Research and a Markey Scholarship to M.M., and a Research Assistantship from the Harvard-MIT Division of Health Sciences and Technology to S.S.

Correspondence and requests for materials should be addressed to M.M. (e-mail: meister@biosun.harvard.edu).